

# Glomerular Maps without Cellular Redundancy at Successive Levels of the *Drosophila* Larval Olfactory Circuit

Ariane Ramaekers,<sup>1</sup> Edwige Magnenat,<sup>1</sup>  
Elizabeth C. Marin,<sup>2</sup> Nanaë Gendre,<sup>1</sup>  
Gregory S.X.E. Jefferis,<sup>2,3</sup> Liqun Luo,<sup>2,3</sup>  
and Reinhard F. Stocker<sup>1,\*</sup>

<sup>1</sup>Department of Biology  
University of Fribourg  
Chemin du Musée 10  
CH-1700 Fribourg  
Switzerland

<sup>2</sup>Department of Biological Sciences  
Stanford University  
Stanford, California 94305

<sup>3</sup>Neurosciences Program  
Stanford University  
Stanford, California 94305

## Summary

**Background:** *Drosophila* larvae possess only 21 odorant-receptor neurons (ORNs), whereas adults have 1,300. Does this suggest that the larval olfactory system is built according to a different design than its adult counterpart, or is it just a miniature version thereof?

**Results:** By genetically labeling single neurons with FLP-out and MARCM techniques, we analyze the connectivity of the larval olfactory circuit. We show that each of the 21 ORNs is unique and projects to one of 21 morphologically identifiable antennal-lobe glomeruli. Each glomerulus seems to be innervated by a single projection neuron. Each projection neuron sends its axon to one or two of about 28 glomeruli in the mushroom-body calyx. We have discovered at least seven types of projection neurons that stereotypically link an identified antennal-lobe glomerulus with an identified calycal glomerulus and thus create an olfactory map in a higher brain center.

**Conclusions:** The basic design of the larval olfactory system is similar to the adult one. However, ORNs and projection neurons lack cellular redundancy and do not exhibit any convergent or divergent connectivity; 21 ORNs confront essentially similar numbers of antennal-lobe glomeruli, projection neurons, and calycal glomeruli. Hence, we propose the *Drosophila* larva as an “elementary” olfactory model system.

## Introduction

Olfactory systems create representations of the odorous environment in the brain. Dissecting the organizational principles of the neural circuits involved has greatly advanced our understanding of how the brain fulfills this amazing task. Breakthroughs in deciphering olfactory circuits were achieved upon the identification of odorant receptors (ORs) and their expression patterns [1–7]. Remarkably, these studies corroborated

earlier predictions that the olfactory systems of mammals and insects are similarly organized [8, 9].

Odorant detection in *Drosophila*, a widely studied olfactory model, relies on 1,300 odorant-receptor neurons (ORNs) [10], each of which expresses essentially a single OR [4, 5, 11, 12]. Axons of ORNs expressing a given OR converge on one or two of 43 invariant glomeruli [13] of the antennal lobe (AL) [6, 7, 14]. Hence, the chemical information conveyed by ORNs is translated into a pattern of glomerular activation [15–18]. This design is very similar to the one previously identified in mammals [19], except that the mammalian system comprises millions of ORNs and thousands of glomeruli [8]. Insect glomeruli are interconnected by a network of local, modulatory interneurons (LNs) [16, 20–22] and are connected via projection neurons (PNs) with second-order olfactory centers, the mushroom body (MB) calyx, and the lateral horn (e.g., [23]). The terminal patterns in the lateral horn are stereotypic, indicating that the map generated in the AL may be retained in modified form therein [24–26].

Very little is known about larval olfactory systems [27]. Adults and larvae of holometabolous insects are morphologically divergent, reflecting their different lifestyles. Adult *Drosophila* display complex behaviors, including foraging, mating, and egg-laying, which require sophisticated odor analysis. Fly larvae, in contrast, live on their food source and do not need long-range odor detection. Although larvae respond to a variety of chemicals [28–32], one may expect their olfactory system to be much simpler. Indeed, odor detection in the larva is accomplished by no more than 21 ORNs ([30], Domingos, A.I., and Vosshall, L.B., 2002 Abstr. Dros. Res. Conf. 43, 783C), which are collected in a single sensillum [33]. In contrast, the 1,300 adult ORNs innervate about 600 individual sensilla [10]. Does this disparity imply that the larval olfactory system is built according to a different design than its adult counterpart, or is it just a miniature version with the same basic organization?

Here we investigate the connectivity of the larval olfactory circuit at cellular resolution by using FLP-out [25] and MARCM [34] labeling. We have previously shown that the 21 ORNs send their axons to the larval antennal lobe (LAL) [35], that GABAergic LNs establish lateral connections within the LAL, and that cholinergic PNs link the LAL with the MB calyx and the lateral horn, all of which is reminiscent of the adult stage [36, 37]. However, comparing adult and larval olfactory circuits requires information about the numbers and connectivity of individual neurons. We demonstrate here that each of the 21 ORNs projects to one of 21 distinct glomeruli of the LAL. Furthermore, the terminals of PNs in the larval MB calyx are restricted to about 28 glomerulus-like domains. Many of the PNs connect one identified LAL glomerulus to one identified calycal glomerulus, creating an olfactory map in a second-order olfactory center. In summary, the larval olfactory pathway shows a strong overall similarity to the adult design but is organized in a numerically much reduced and almost completely

\*Correspondence: reinhard.stocker@unifr.ch

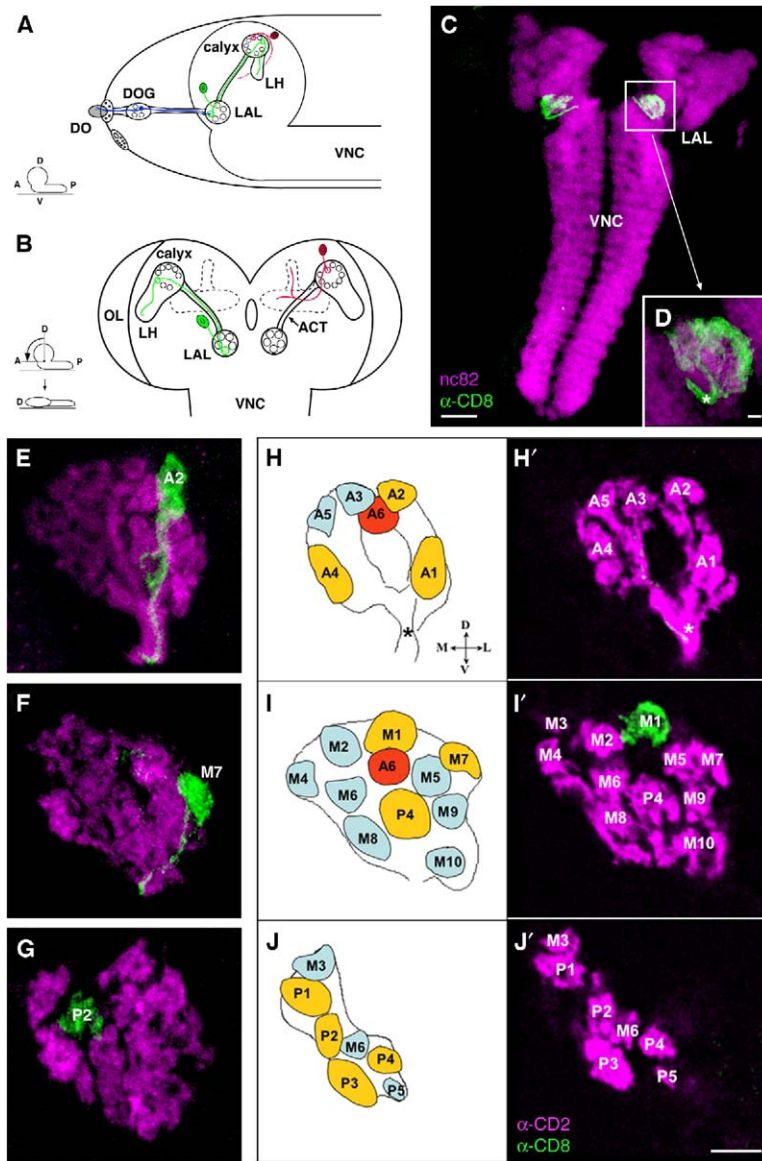


Figure 1. Odorant-Receptor Neurons Establish a Glomerular Map in the Larval Antennal Lobe

(A) Diagram of the larval olfactory system of *Drosophila* (lateral view). Dendrites of the 21 ORNs (one is shown in blue) extend into the central dome sensillum (gray) of the dorsal organ (DO). ORN cell bodies are collected in a ganglion (DOG) and send their axon into the larval antennal lobe (LAL). PNs (green) connect the LAL with the mushroom-body (MB) calyx and the lateral horn (LH). An intrinsic MB neuron is shown in red. The inset indicates anterior (A), dorsal (D), posterior (P), and ventral (V) positions of the CNS. VNC: ventral nerve cord.

(B) Diagrammatic view of a flattened preparation, in which the brain has been rotated by 90° relative to the VNC (inset). Thus, the A/P axis of the brain becomes the Z axis in the confocal microscope. All figures shown hereafter derive from flattened preparations. MB lobes are shown by dotted lines. ACT: antennocerebral tract, OL: optic lobe.

(C and D) The OR83b-GAL4 line, driving expression in 20 of the 21 ORNs, reveals projections of olfactory afferents in the LAL (green: CD8 reporter expression; magenta: nc82 neuropil staining). (C) Confocal stack of entire larval CNS. (D) Higher magnification of LAL showing entrance of the antennal nerve (asterisk).

(E–G) Projections of single ORNs visualized by FLP-out. OR83b-GAL4-positive ORNs that underwent FLP-mediated recombination express CD8 (green), whereas the rest express CD2 (magenta). Single ORNs invariably send their axon to a single glomerulus. Mutually exclusive expression domains of CD2 and CD8 demonstrate that each glomerulus is the target of a single OR83b-positive axon (cf. Figure S1). All panels represent stacks of multiple confocal sections, resulting in the white appearance of the axon in (E).

(H–J') ORN projections allow one to establish a glomerular map of the LAL, displayed at anterior (H and H'), middle (I and I'), and posterior (J and J') levels (cf. Figure S2). Schematic representations (H, I, and J) and

corresponding confocal stacks of a single LAL (H', I', and J') showing the site of 21 individual glomeruli. Anterior, middle, and posterior glomeruli are termed A1–A6, M1–M10, and P1–P5, respectively. Ten landmark glomeruli (yellow and red) are relatively invariant in size, shape, and position; more-variable glomeruli are shown in blue. A6 (red) was identified only by PN dendritic arborization (cf. Figures 2E and 2F), suggesting that it may be the target of the unique OR83b-negative ORN. The spatial orientation for panels (E–J') is given in panel (H). Asterisks on (H) and (H') indicate the entrance of the antennal nerve. The scale bars represent 25 μm (C), 5 μm (D and J'); the bar in (J') corresponds to panels (E–J').

nonredundant way, leading to a simple 1:1:1:1 relationship among ORNs, LAL glomeruli, PNs, and calycal glomeruli. Hence, we propose the *Drosophila* larva as an “elementary” olfactory model system.

## Results

### Projections of Odorant-Receptor Neurons Establish a Glomerular Map in the Larval Antennal Lobe

The key features of the larval olfactory system and the appearance of the olfactory circuit in flattened brain preparations are shown in Figures 1A and 1B, respectively. The cell bodies of the 21 larval ORNs are collected in a ganglion below the dome sensillum, which

forms part of the dorsal organ (Figure 1A). ORN afferents project into the LAL, which was previously shown to consist of distinct subregions [36]. To address whether these subregions are analogous to the glomeruli of the adult AL, we asked if larval ORN terminals extend throughout the entire LAL or whether, as in adults, ORNs are defined by particular target glomeruli.

ORN projections in the LAL were visualized with an OR83b-GAL4 line [16] (Figures 1C and 1D) that we found to be expressed in 20 of the 21 larval ORNs. Using the FLP-out method [25], we labeled individual ORNs by the CD8-GFP marker, against the background of the remaining GAL4-expressing ORNs labeled by CD2. The axonal projection patterns of single and double

ORN clones ( $n = 72$  and  $n = 6$ , respectively) labeled by FLP-out during late embryogenesis (18–24 hr after egg laying [AEL]) were studied in early third-instar larval brains (72–78 hr AEL). We found that the 20 OR83b-expressing ORNs define 20 discrete target subregions, termed provisionally “glomeruli,” in the LAL. Significantly, each single ORN projection is restricted to a single glomerulus ( $n = 72/72$ ) (Figures 1E–1G). Correspondence between the numbers of labeled ORNs and glomeruli suggested that each ORN projects to a specific glomerulus. In FLP-out clones, any single cell can either express CD8 or CD2, but never both markers [25]. Thus, if a given glomerulus is the target of a single ORN, ORN clones should label individual glomeruli exclusively by CD8 but not by CD2. Indeed, in none of the 84 glomeruli (from 78 hemibrains) innervated by individually labeled ORNs did CD8 and CD2 expression overlap (Figures 1E–G and 1I'; also Figure S1 available with this article online).

The glomerular pattern among different individuals was quite conserved with regard to their relative size, shape, and position and displayed bilateral symmetry. This allowed us to use ORN projections to establish an annotated glomerular map of the LAL (Figures 1H–1J' and Figure S2). Among the 20 glomeruli recognized, nine exhibited invariant size, shape, and position and were classified as landmark glomeruli (A1, A2, A4, M1, M7, P1, P2, P3, P4). An additional twenty-first glomerulus (landmark A6) was revealed by the dendritic arborization pattern of PNs (see below). Glomerulus A6 may be the target region of the one ORN not labeled by OR83b-GAL4. Taken together, ORNs seem to establish a straightforward LAL map comprising 21 primary “olfactory identities.”

#### Arborizations of Local Interneurons Cover the Entire Larval Antennal Lobe

To study arborization patterns of individual LNs [36], we generated FLP-out clones in the *c739-GAL4* driver line [38] that we found to be expressed in a subset of approximately 21 larval LNs. Their cell bodies are arranged within three groups, ventro-lateral, lateral, and dorsal to the LAL, encompassing about ten, six and five neurons, respectively (Figure 2A). The single and double LN clones generated ( $n = 7$  and  $n = 3$ , respectively) all belonged to the ventro-lateral cluster. We found that, as with the most frequent type of adult LNs, arbors of these LNs covered the entire LAL (Figure 2B).

#### Projection Neurons Establish Dendritic Arborizations in Single Glomeruli of the Larval Antennal Lobe

To determine whether the dendrites of the larval PNs respect the organization of ORN projections in the LAL, we used the GH146-GAL4 driver, which is expressed by about 90 of an estimated 150 adult PNs [25, 39]. In the third-instar larva, GH146 labels 16–18 mature larval PNs [40] from an unknown total. Their somata are located antero-dorsally to the LAL, and their axons project via the antennocerebral tract to the MB calyx and the lateral horn, as do those of their adult homologs [36] (Figures 1A, 1B, 2C, and 2D). In addition, GH146 is expressed in two clusters of immature PNs, sitting antero-dorsal and lateral to the LAL [41] (Figures 2C and 2D).

These adult-specific PNs, which still lack dendrites and axon terminals, were not studied here.

By performing FLP-out in GH146-GAL4, we generated 50 single and 25 double clones of mature PNs in early third-instar larvae. Their dendritic arbors were invariably confined to single LAL glomeruli (Figures 2E–2G). In a study of MARCM clones, 16% of the labeled PNs were recently observed to target two glomeruli of the LAL [40] (for discussion of the two techniques, see the Supplemental Data). By comparing the shape, size, and position of PN dendritic fields with the pattern of afferent terminals (Figures 1E–1J'), we confirmed that the glomeruli formed by the GH146-positive PNs correspond to ORN target glomeruli (Figures 2E–2G). As shown above, an additional glomerulus A6 was detected with GH146 (Figures 2E and 2F; cf. Figures 1H and 1I). Interestingly, in all 75 PN FLP-out clones studied, the glomeruli visualized by CD8 were devoid of CD2 labeling (Figures 2E–2G and S1). Therefore, unlike in the adult, each glomerulus seems to be innervated by a single GH146-positive PN. Even though the GH146 pattern does not comprise all PNs, redundancy (if any) in PN innervation of the different LAL glomeruli must be low.

#### Most Larval Projection Neurons Target Single Glomeruli in the Mushroom-Body Calyx

When studying PN output regions, we noticed scattered *n-syb-GFP* reporter expression [42] driven by GH146 in the LAL (Figures 3A and 3B). Because no other GH146-positive cells projecting to the LAL were detected, this suggests the presence of presynaptic domains in PNs inside the LAL. Such circuitry would not be surprising, given that the presynaptic sensor synapto-pHluorin is expressed in PNs in the adult AL [16]. Intraglomerular PN dendrodendritic synapses identified in *Manduca* [43] have been postulated to mediate LN-independent lateral inhibition [21].

The dominant outputs of PNs are located in the MB calyx and the lateral horn. We focused our study on the calyx because the axon terminals in the lateral horn were difficult to classify as a result of the lack of suitable landmarks. In the adult calyx comprising hundreds of glomeruli [44], the branching patterns of individual PNs do not present an obvious stereotypy [24, 25]. Yet, concentric calycal zones that correspond to subsets of PNs defined by their input glomeruli in the AL were observed [26]. The larval calyx, an elaborate hemispheric structure, is made of a small number of glomerulus-like substructures (referred to as calycal glomeruli) [40]. Analysis of confocal stacks stained by choline acetyltransferase (ChAT) immunoreactivity alone, or in combination with GH146-driven *n-syb-GFP* or CD8, revealed the presence of about 28 glomeruli (mean = 28.3;  $n = 8$ ), all of which occupy the peripheral layer of the calyx (Figures 3C and 3D). Eighteen to 23 of them (mean = 19.9;  $n = 8$ ) were found to be targets of GH146-positive PNs; the others are probably innervated by GH146-negative PNs. In addition, GH146-positive boutons lacking  $\alpha$ -ChAT immunoreactivity were observed in the center of the calyx (Figures 3C and 3D). These terminals could correspond either to PNs or to a few additional GH146-positive neurons projecting to the calyx (data not shown). Studying the same PN clones as we did for

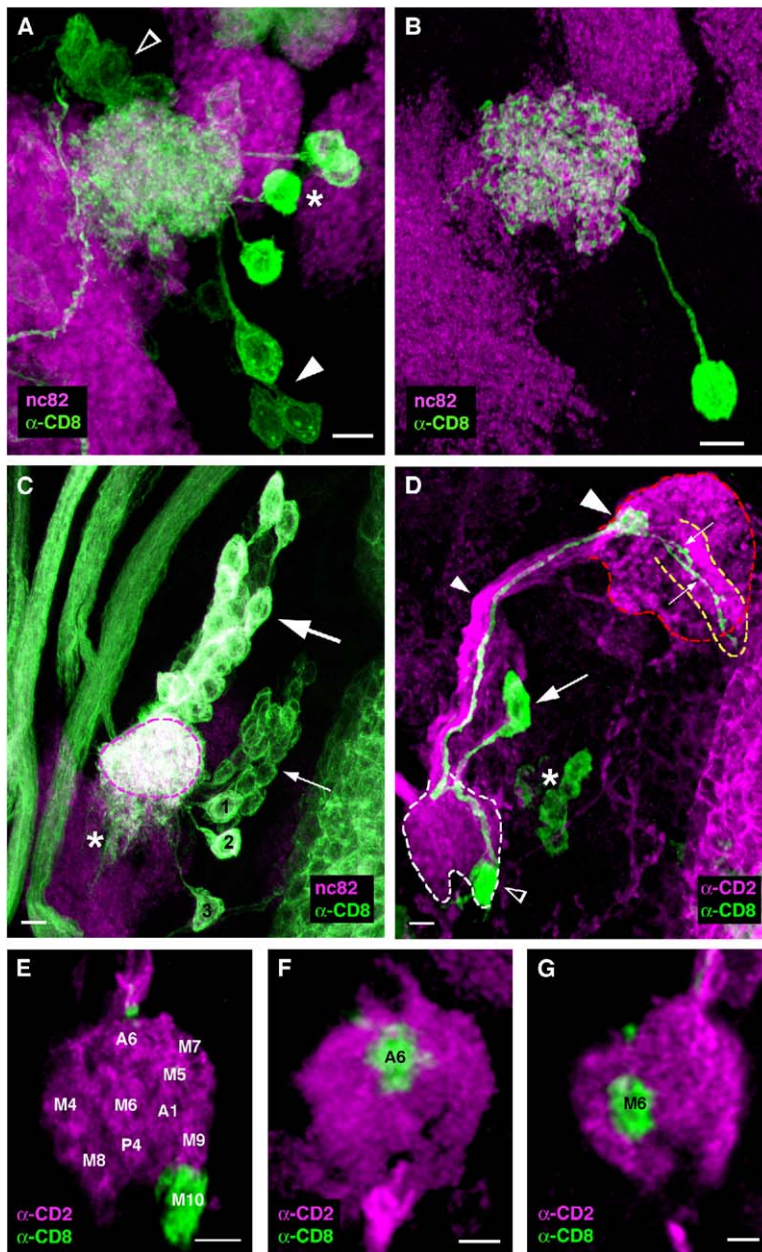


Figure 2. Anatomy of Larval Local Interneurons and Projection Neurons

(A) The approximately 20 LNs labeled by the c739 GAL4 line (green) have their cell bodies ventro-lateral (filled arrowhead), lateral (asterisk), or dorsal (open arrowhead) of the LAL.

(B) FLP-out in c739 shows arborizations of just one ventro-lateral LN in the entire LAL.

(C) The GH146-GAL line visualized by CD8 (green) is expressed by two clusters of PNs. The antero-dorsal cluster (large arrow) comprises 16–18 larval PNs and some immature adult PNs; the lateral cluster (thin arrow) includes only immature PNs. Three other neurons (1–3) unrelated to the LAL (dashed contour) establish dendrites in the suboesophageal ganglion (asterisk).

(D) Single GH146-positive PN (arrow) labeled via FLP-out by CD8 (green) on top of other PNs (and additional GH146-positive cells) labeled by CD2 (magenta). The PN establishes dendritic arbors in a single glomerulus (empty arrowhead) of the LAL (white contour). Its axon follows the antennocerebral tract (small filled arrowhead), forms a glomerular-type terminal (large filled arrowhead) in the MB calyx (red contour), and extends farther (thin arrows) into the lateral horn (yellow contour). The asterisk indicates a subset of immature PNs expressing CD8.

(E–G) Dendritic patterns of single PNs labeled by CD8 (green) via FLP-out; the remaining GH146-positive PNs express CD2 (magenta). Similar to ORN terminals, dendrites of single PNs arborize within single LAL glomeruli. CD2 and CD8 expression domains are mutually exclusive, indicating that each glomerulus is innervated by a single GH146-positive PN (cf. Figure S1). Glomeruli recognized by PN dendrites coincide with those identified for ORN terminals (cf. terminology on panels [E–G] with the one in Figures 1H–1J’).

All images represent stacks of confocal sections, with dorsal on top and lateral to the right. Scale bars represent 5  $\mu$ m.

the LAL showed that, in general, individual PNs choose single calycal glomeruli as targets (Figures 3E and 3F). However, in four out of the 100 labeled cells, PNs established arborizations in two calycal glomeruli (Figure 3G). In a study of MARCM clones, 29% of PNs were found to target two calycal glomeruli [40] (for discussion of frequencies, see the Supplemental Data). The slightly higher number of calycal glomeruli compared to LAL glomeruli could be at least partially related to this subtle type of PN divergence. In all FLP-out clones, PN terminals in the calyx expressed either CD8 or CD2 (Figures 3E and 3F, and S1), suggesting that calycal glomeruli are innervated by a single GH146-positive PN.

On the basis of the combination of  $\alpha$ -ChAT and GH146-CD2/CD8 labeling, we were able to establish an annotated glomerular map of the larval calyx (Figures

3H–3J’). Among the total of about 28 calycal glomeruli, only those 24 that were identifiable in all preparations were included in the map. Nine (a6, m1, m5, m7, m9, p2, p3, p4, p7) showing a particularly invariant size, shape, and position were classified as landmark calycal glomeruli. The four calycal glomeruli not included in the map were mostly located in an ill-defined calycal area connected to the lateral horn (Figure 3H’).

#### Stereotypical Connectivity of Larval Projection Neurons

We next compared the input and output glomeruli of the 50 single PN clones. Remarkably, 24 of them fell into seven PN types connecting specific LAL glomeruli with specific calycal glomeruli (Figure 4; Table 1). Thus, at least part of the calyx seems to receive a spatial

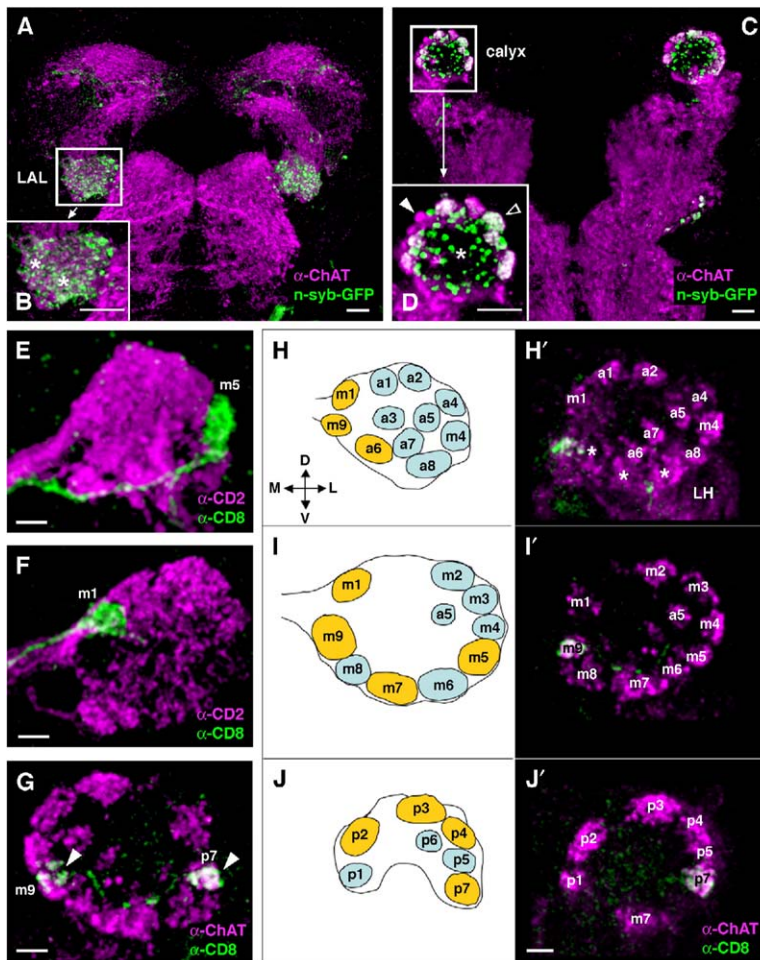


**Figure 3. Terminals of Projection Neurons in the Mushroom-Body Calyx Respect Glomeruli Borders**

(A and B) The LAL of the GH146-GAL4 line exhibits scattered n-syb-GFP reporter expression (green), which is probably located in PN dendrites (asterisks in [B]).

(C and D) The periphery of the MB calyx is characterized by glomeruli-like subregions that are strongly immunoreactive to  $\alpha$ -ChAT. Most of these glomeruli comprise dense terminals of GH146-positive PNs ([D], open arrowhead, white overlap), but others do not ([D], filled arrowhead). n-syb-positive domains are also localized in the center of the calyx ([D], asterisk), but they do not coincide with  $\alpha$ -ChAT expression (see text).

(E and F) Terminals of single GH146-positive PNs labeled via FLP-out by CD8 (green) in the background of other GH146-positive PNs (CD2: magenta) demonstrate that different PNs project to different calycal glomeruli. Mutually exclusive expression of CD2 and CD8 indicates that these glomeruli are targets of single GH146-positive PNs (cf. Figure S1).

(G) As shown by a single-cell FLP-out (green) on top of  $\alpha$ -ChAT immunocytochemistry (magenta), a PN may sometimes innervate two calycal glomeruli (arrowheads).

(H–J') Glomerular map of the larval MB calyx, displayed at anterior (H and H'), middle (I and I'), and posterior (J and J') levels. Schematic representations (H, I, and J) and corresponding confocal stacks of a single calyx stained by  $\alpha$ -ChAT immunocytochemistry (H', I', and J'), magenta) showing 24 annotated glomeruli. Anterior, middle, and posterior calycal glomeruli are termed a1–a8, m1–m9, and p1–p7, respectively. Landmark glomeruli are shown in yellow, less obvious

glomeruli in blue. Glomeruli m9 (I') and p7 (J') are targets of a GH146-positive PN labeled by FLP-out (white overlap). Additional glomeruli are present in an ill-defined region of the calyx (H', asterisks) close to the lateral horn (LH). The spatial orientation for panels (E–J') is provided in panel (H).

All confocal images represent stacks of multiple sections; scale bars represent 10  $\mu$ m (A–D) and 5  $\mu$ m (E–G and J'); the bar in (J') corresponds to panels (H–J').

representation of the olfactory world via this stereotyped PN input. The map generated in the calyx does not directly reflect the spatial relations of the LAL glomeruli involved, although anterior, middle, and posterior levels of the LAL tend to be connected to corresponding levels in the calyx (five of the seven PN types). We cannot exclude the possibility that some PNs innervate variable input and output regions, but we never observed PNs that unequivocally connected a particular glomerulus in one structure with more than one possible glomerulus in the other. Taken together, the general impression is that of a stereotyped and spatially organized transfer of information from the LAL to the MB calyx.

### Mushroom-Body $\gamma$ Neuron Connectivity in the Larval Calyx

In the larval calyx, PNs synapse mostly with the  $\gamma$  type of intrinsic MB neurons;  $\gamma$  neurons are born during embryonic and early larval life [40]. To study their connectivity, we analyzed 115 single and two cell MARCM

clones by using the drivers 201Y [38] and OK107 [45], as well as 11 FLP-out clones (encompassing 15 MB  $\gamma$  neurons) labeled by the MB247 driver [46, 47]. Because brains were studied at the middle to late third larval instar, the mature MB neurons visible were of the  $\gamma$  neuron type [48]. Roughly 25% of the MB  $\gamma$  neurons labeled by MARCM before larval hatching ( $n = 20/82$ ), and all MB  $\gamma$  neurons analyzed by FLP-out (induced 42–85 hr AEL), had dendrites in a single calycal glomerulus (Figures 5A and 5B). About 40% of the MARCM clones projected to two or three glomeruli ( $n = 33/82$ ) (Figures 5C and 5D), 20% of them had diffuse dendrites in a substantial volume of the calyx ( $n = 16/82$ ) (Figures 5E and 5F), and the remaining 15% ( $n = 13/82$ ) had sparse processes that extended deep in the calyx and did not appear to target any specific glomeruli. Similar to an earlier report [48], MB  $\gamma$  neuron MARCM clones labeled by heat shock from 0 to 52 hr after larval hatching always had sparse dendritic projections distributed throughout the calyx and never exhibited uniglomerular or biglomerular dendrites ( $n = 33/33$ ) (not shown). Thus, although MB  $\gamma$  neurons are generated continuously

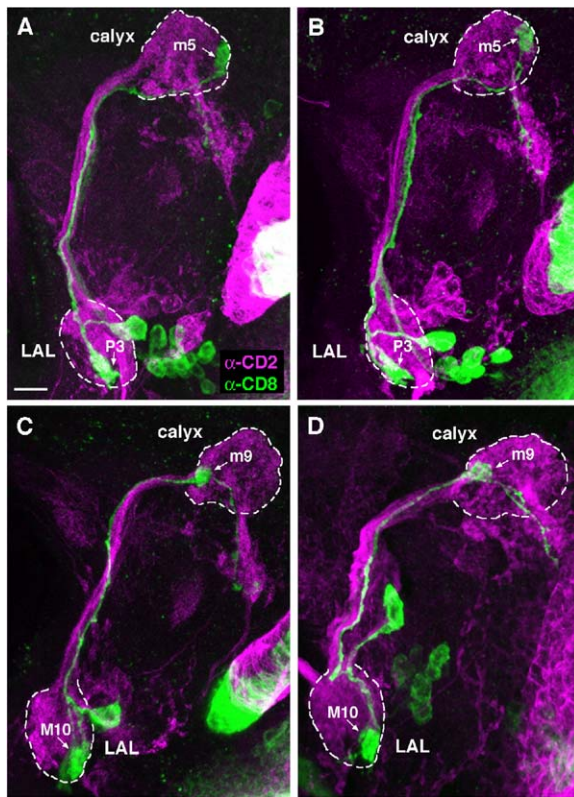


Figure 4. Subsets of Projection Neurons Establish a Spatial Map in the Larval Mushroom-Body Calyx

Single-cell FLP-outs in GH146-GAL4 suggest that many PNs are identifiable with respect to their input glomeruli in the LAL and output glomeruli in the MB calyx (cf. Table 1). The panel pairs (A and B) and (C and D) show two different types of PNs from two individuals each, exhibiting a specific input and output pattern in the glomeruli indicated. PNs that underwent FLP-out express CD8 (green), whereas the remaining PNs express CD2 (magenta). All panels represent stacks of multiple confocal sections, with dorsal on top and lateral to the right. The scale bar represents 10  $\mu\text{m}$  (A–D).

throughout early development [48], those generated before and after larval hatching are morphologically distinct. The diffuse arborization types seen in some of the “embryonically induced” MARCM clones could even be explained by delayed, postembryonic recombination due to perdurance effects. On the other hand,

Table 1. Identification of Distinct Types of Larval Projection Neurons

LAL Glomerulus	Calycal Glomerulus	n
M10	m9	6
P3	m5	5
A2	a6	3
M7	p4	3
M9	m3	3
P2	p6	2
P5	p2	2

The seven identified types of larval PNs are characterized by distinct input glomeruli in the LAL and output glomeruli in the MB calyx. Glomerular terminology follows Figures 1 and 3. n = number of independent single PN clones analyzed.

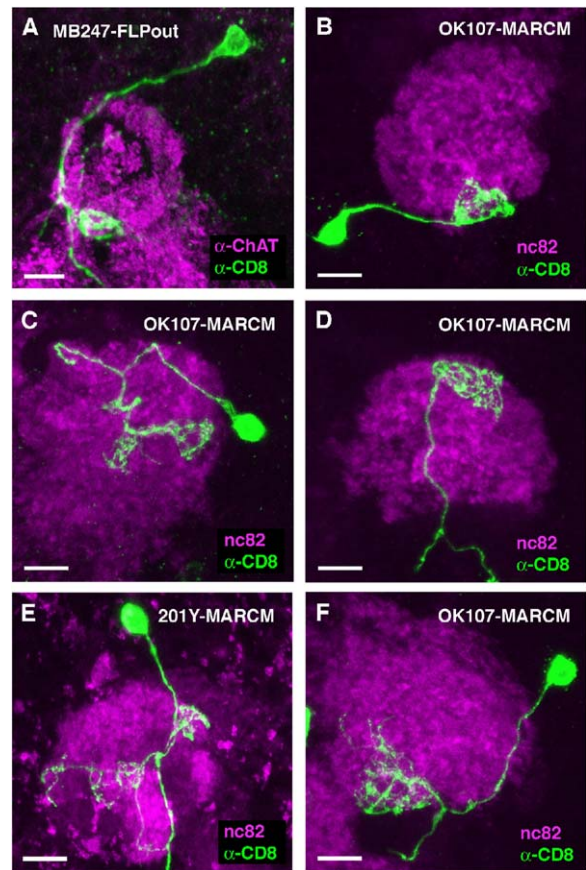


Figure 5. Dendritic Connectivity of Mushroom-Body  $\gamma$  Neurons in the Larval Calyx

FLP-out (A) and MARCM clones (B–F) reveal different types of MB  $\gamma$  neurons in the larval calyx. Dendritic arbors may be present in a single calycal glomerulus (A and B), in two glomeruli (C and D), or in larger calyx areas (E and F). The patterns shown are based on three different driver lines, MB247-GAL4, OK107-GAL4, and 201Y-GAL4. All panels represent stacks of multiple confocal sections, with dorsal on top and lateral to the right. Scale bars represent 5  $\mu\text{m}$ .

the fact that all of the MB  $\gamma$  neurons induced by FLP-out were of the uniglomerular type suggests that they were born during embryogenesis.

## Discussion

Here we analyze the organizational logic of the larval olfactory pathway in *Drosophila* (Figure 6). We show, at the single-cell level, that the projections of each of the 21 ORNs in the LAL segregate and uniquely target one of 21 glomeruli. Moreover, PNs are also organized in a glomerular fashion, both at their input level in the LAL and at one of their output regions, the MB calyx. The overall invariance of glomeruli both in the LAL and calyx allowed us to create annotated glomerular maps for both of these olfactory centers. Based on these maps, we were able to extract a surprisingly high degree of stereotypy in the connectivity between defined LAL glomeruli and calycal glomeruli. This suggests a transfer of the glomerular map of the LAL in modified form to the

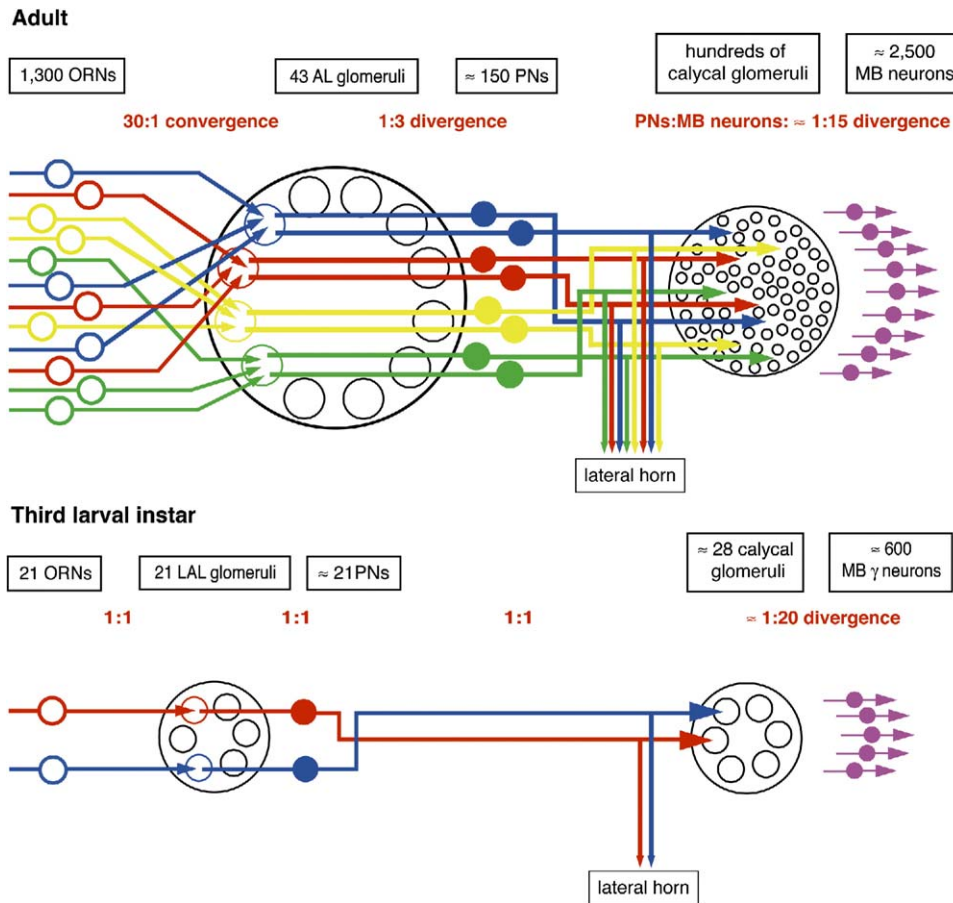


Figure 6. Wiring Diagram: Adult versus Larval Olfactory System of *D. melanogaster*

Adult and larval olfactory pathways share the same general design. However, there are twice as many primary “olfactory identities” (ORN types or AL glomeruli, shown in different colors) in the adult. Moreover, in the adult AL, the different types of ORNs (open circles) and PNs (filled circles) that innervate a particular AL glomerulus occur in multiple copies, whereas larval ORN and PN types are unique, resulting in an almost complete lack of cellular redundancy. Thus, the adult olfactory pathway is characterized by converging and diverging connectivity in the AL, whereas the larval pathway is organized as straightforward channels in which ORNs, LAL glomeruli, PNs, and calyca glomeruli are related essentially in a 1:1:1:1 fashion (ratios indicated in red refer to the features shown in the preceding line). The larval MB calyx retains a strong spatial organization that is not obvious in the adult (note: adult MBs include, apart from MB  $\gamma$  neurons, additional classes of intrinsic neurons).

MB calyx. We finally demonstrate that the MB  $\gamma$  neurons, the PN target neurons in the calyx, fall into a number of distinct classes according to their dendritic patterns in the calyx. Our data reveal both similarities and differences with the organization of the adult olfactory circuit (Figure 6) and invite interesting speculations about olfactory coding.

#### Organization of the Larval Antennal Lobe, the Primary Olfactory Association Center

We demonstrate that the 21 identifiable glomeruli of the LAL are the structural units recognized by the terminals of ORNs and the dendritic domains of PNs. Hence, the glomeruli of the LAL meet the wiring criteria of typical insect glomeruli. Because of the lack of overlap of CD8 and CD2 labeling in PN FLP-out clones, we conclude that each LAL glomerulus (apart from being a target of a single ORN) is innervated by a single GH146-positive PN. If this condition applies to the remaining, GH146-

negative PNs, the total PN number should be 21; even if it does not, cellular redundancy at the level of PNs is obviously rather low.

The organizational logic of the larval olfactory pathway depends on whether larval ORNs express a single type of OR, as in the adult fly and in mammals, or multiple ORs, as in *C. elegans* [49]. Recent studies suggest that *Drosophila* larval ORNs express only one or two ORs in addition to the ubiquitously expressed OR83b and thus resemble the adult system (L. Vosshall, personal communication, and [50]). This type of expression appears to be in agreement with the organization of ORN and PN projections as parallel channels and is further supported by behavioral studies demonstrating that *Drosophila* larvae are able to discriminate among various odorants [28, 29, 31, 32]. Hence, the binding of an odorant to a subset of larval ORs would be translated into a specific pattern of activated glomeruli in the LAL. Given that there are 21 LAL glomeruli, the

larval olfactory world seems to be characterized by 21 primary olfactory identities (cf., [51, 52]).

Although our data prove that LAL glomeruli are targets of single ORNs, they do not allow us to determine whether a specific glomerulus is “recognized” by a given ORN. It would be possible to answer this question by mapping projections of ORNs expressing a particular OR. Yet, a circumstantial indication about the specificity of ORN projections is provided by the invariant position of A6, the only unlabeled glomerulus of the OR83b-GAL4 driver used.

Whereas, in the adult, three to five morphologically identical PNs innervate the same AL glomerulus [39], a single larval PN appears to correspond to each LAL glomerulus. According to the simplest coding rule, the spatial pattern of glomerular activation could be directly transferred from a specific subset of ORNs to the corresponding subset of PNs, maintaining the parallel ORN channels as labeled PN lines. However, the presence of LNs in the LAL suggests that the signals provided by the ORN inputs may undergo some transformation, in agreement with physiological data from larval PNs in *Manduca* [27]. Analyzing this issue in the adult AL of *Drosophila* and other insects has led to somewhat contradictory results [16, 17, 21, 22, 53]. However, there is consensus about lateral glomerular interactions provided essentially by LNs. Similar processing could occur also in the larva; we have shown that larval LNs may interconnect most or all glomeruli.

#### Organization of the Mushroom-Body Calyx, a Second-Order Olfactory Center

We show that the larval MB calyx is a spherical structure composed of about 28 glomeruli. The vast majority of PNs project into a single calycal glomerulus, whereas a few terminate in two glomeruli. More importantly, we demonstrate a surprising degree of stereotypy in the projections of PNs to the calyx. We have identified seven PN types that connect a given LAL glomerulus with a defined calycal glomerulus. Thus, at least a subset of larval PNs is involved in transferring the activity pattern in the LAL faithfully to the next level of the olfactory pathway. Because of methodological limitations, we cannot rule out the possibility that the input-output relations of certain larval PNs are variable. Nevertheless, the PN outputs in the larval calyx are organized differently than in adult PNs, which establish from one to 11 boutons in variable calyx regions [25], each of these boutons probably corresponding to a single glomerulus [44]. Moreover, single-cell analysis of adult PN projections failed to demonstrate a precise patterning of terminals in this area [24, 25]. Although concentric target zones could be defined for PNs deriving from specific AL glomeruli [26], these zones are quite distinct from the precise glomerular terminations of larval PNs. The straightforward connectivity of the latter seems well suited for analyzing calyx function.

Our data demonstrate that embryonic-born MB  $\gamma$  neurons, similar to adult MB neurons [54], fall into several classes according to their dendritic arbors in the larval calyx: uniglomerular and biglomerular neurons and neurons exhibiting diffuse dendrites within larger domains of the calyx. These different classes suggest alternative

ways in which olfactory information may be processed in the larval MB. In the first, the activity pattern established in the LAL would be transferred in a one-to-one manner, with each uniglomerular MB  $\gamma$  neuron receiving input from one PN. Hence, the parallel channels established in the ORNs and PNs would continue in the MBs, leading to an elementary coding of odor features. The second pathway would be combinatorial, with each multiglomerular MB  $\gamma$  neuron receiving inputs from two or more PNs and thus acting as a coincidence detector for interpreting their combined activity as an odor [55, 56]. The various wiring types observed suggest that both principles may occur together. Also, the fact that perhaps 25–30 PNs connect to an estimated 600 functional larval MB neurons in the middle third larval instar demonstrates that calycal glomeruli are principal sites of divergence, as in the adult [44].

#### The Larval Olfactory System of *Drosophila*: Functional Considerations

The main features of the larval olfactory system in terms of cell types and their target regions are obviously similar to those of the adult. Yet, the numbers of neurons that constitute the larval olfactory pathway up to the MB calyx are strongly reduced. In fact, every neuron in this system appears to be unique, leading to an almost complete lack of cellular redundancy. Therefore, we propose the larval olfactory system of *Drosophila* as an elementary model for olfactory studies; it is a system that still possesses the essential design of the mammalian olfactory system, but in the simplest form. Its usefulness as a model is strengthened by an obvious consequence of the cellular nonredundancy; any loss of ORNs and PNs can be predicted to affect olfactory function more severely than in the adult system.

The simplicity of the larval olfactory pathway includes two additional aspects: the low number of parallel channels and the lack of convergent and divergent connectivity in the LAL (Figure 6). The presence of only 21 different types of ORNs and LAL glomeruli obviously reduces the number of primary olfactory channels by more than half in comparison to the adult. Moreover, given the uniglomerular patterns of ORNs and PNs in the LAL, the almost equal numbers of ORNs, LAL glomeruli, and PNs result in the lack of convergent and divergent connectivity in the LAL. Whereas in the adult olfactory pathway 1,300 ORNs converge onto about 50 glomeruli, which diverge again to approximately 150 PNs and hundreds of calycal glomeruli, the larval pathway is organized essentially in a 1:1:1:1 manner. Convergence of many sensory fibers onto a few target neurons, a principle found in numerous systems, increases the signal-to-noise ratio. Thus, the lack of sensory convergence together with the low number of ORN types is likely to make the larval system less sensitive than the adult system, both quantitatively and qualitatively. On the other hand, divergent connections, such as those observed between AL glomeruli and PNs in the adult, expand the signals to a wider array of channels after the signals are initially processed. Thus, the lack of expansion along the larval olfactory pathway is expected to further reduce the capacity of the larval system. Taken together, the odor-detection system of the

larva is likely to be less sensitive than its adult counterpart. However, it may still be adequate for an animal that lives on its food supply. A careful comparative study of the olfactory capacities of the two stages would be required to test this hypothesis.

In summary, the larval olfactory circuit of *Drosophila* shows a strong overall similarity to the adult design, but it is organized in a numerically much reduced and almost completely nonredundant way. In particular, there is a simple 1:1:1:1 relationship among ORNs, LAL glomeruli, PNs, and calycal glomeruli and an absence of convergent and divergent connectivity in the LAL. Hence, we propose the *Drosophila* larva as a “minimal” model for studying olfactory coding.

## Experimental Procedures

### Fly Strains

Flies were raised on standard medium at 25°C. The strains *y w*; OR83b-GAL4 [16], *y w*67c23;c739 [38], and GH146-GAL4 [39, 57] were used to label ORNs, LNs, and PNs, respectively. For labeling of MB  $\gamma$  neurons, three lines were utilized, MB247 [46, 47], OK107 [45], and 201Y [38]. *y w*;UAS-mCD8:GFP/CyO [34] and UAS-n-syb-GFP [42] were used as reporter lines. Flies for the FLP-out clonal analysis [58] were obtained from crosses of males of each of the GAL4 lines cited above with virgin females of the following stock: hsFLP;CyO/Sp;UAS>y+ CD2>CD8:GFP [25].

### Clone Induction

FLP recombinase was induced by heat shock of 1 hr at 35°C [25] at the following developmental stages: 12–24 hr AEL for ORN and PN clones; 25–31 hr AEL for LN clones, and 42–85 hr for MB  $\gamma$  neuron clones. Embryos and larvae were then allowed to develop at 25°C until 72–85 hr AEL (for ORNs, PNs, and MB  $\gamma$  neurons) and 66–72 hr AEL (for LNs), when they were dissected.

MARCM clones [34] in MB  $\gamma$  neurons were induced by heat shock of embryos or larvae of the following genotypes: *y w* hs-FLP UAS-mCD8:GFP(*y w* or *Y*);FRTG13tubP-GAL80/FRTG13 GAL4-201Y UAS-mCD8:GFP or *y w* hs-FLP UAS-mCD8:GFP(*y w* or *Y*);FRTG1-3tubP-GAL80/FRTG13;GAL4-OK107/+. Embryos were collected on grape-juice agar plates at 25°C. For embryonic heat shock, embryos were stored at 16°C before and until 24 hr after the heat shock; the temperature was then raised past 18°C, 20°C, and finally 25°C to prevent accidental hs-FLP induction. For larval heat shock, newly hatched larvae were collected and raised at 25°C until dissection.

### Immunofluorescence and Microscopy

Two alternative protocols modified from [36, 59] were used for dissection, fixation, and immunostaining. In brief, larvae were pre-dissected either in phosphate buffer (PB) (0.1 M, pH 7.2) or in phosphate-buffered saline (PBS) with 0.2% Triton X-100; the brains attached to the body wall were fixed for 20 min in PB containing 4% paraformaldehyde (in PBS) and subsequently rinsed in PBT (0.3% Triton X-100 in PB) or PBS with 0.2% Triton X-100. After 1 hr of preincubation in PBT with 3% or 5% NGS at room temperature, the preparations were incubated with a cocktail of primary antibodies overnight at 4°C. Primary antibodies included nc82 (dilution 1:20) from E. Buchner and A. Hofbauer (Universities of Würzburg and Regensburg, Germany), anti-ChAT (1:500) from P. Salvaterra (Beckman Research Institute, City of Hope, Duarte, CA), anti-CD8 (1:100; Caltag, Burlingame, CA), and anti-CD2 (1:100; Serotec GmbH, Düsseldorf, Germany). After several rinses in PB-Triton X-100 or PBS-Triton X-100, samples were incubated overnight in PBT-NGS with the secondary antibodies (anti-rabbit, anti-rat, highly cross-adsorbed anti-mouse Alexa Fluor (–488 or –568)-conjugated, diluted 1:200 or 1:300; Molecular Probes). After several rinses, brains were detached from the body walls and mounted in Vectashield (Vector Labs) or in glycerol containing Anti-Fade (Molecular Probes), with nail polish used as spacer.

### Image Acquisition and Processing

Stacks of confocal images at 0.5  $\mu$ m to 2  $\mu$ m spacing were collected with a Biorad MRC 1024 confocal microscope and LaserSharp image-collection software. Images were then processed with Image J 1.31 and 1.32 (<http://rsb.info.nih.gov/ij/index.html>), NIH Image 1.62, or Adobe Photoshop software. Volumetric measurements were performed with Imaris (Bitplane AG, Zürich, Switzerland).

### Supplemental Data

Supplemental Data are available with this article online at <http://www.current-biology.com/cgi/content/full/15/11/982/DC1/>.

### Acknowledgments

We thank J.-M. Dura, G. Miesenböck, M. Ramaswami, P. Salvaterra, L. Vosshall, and A. Wong for kindly providing stocks and reagents and N. Grillenzoni for technical support with confocal microscopy. We are grateful to B. Gerber (Würzburg), N. Grillenzoni (Fribourg), and J.P. Rospars (Versailles) for comments and discussions. We appreciate permission by L. Vosshall (New York) for citation of unpublished data. This work was supported by the Swiss National Funds (31-63447.00 and 3100A0-105517: R.F.S.; 3234-069273.02: A.R.), Roche Research Foundation (A.R.), a predoctoral fellowship from the Howard Hughes Medical Institute (E.C.M.), and a National Institutes of Health grant (R01-DC005982: L.L.).

Received: February 17, 2005

Revised: April 12, 2005

Accepted: April 12, 2005

Published online: May 19, 2005

### References

1. Buck, L., and Axel, R. (1991). A novel multigene family may encode odorant receptors: A molecular basis for odor recognition. *Cell* 65, 175–187.
2. Ressler, K.J., Sullivan, S.L., and Buck, L.B. (1994). Information coding in the olfactory system: Evidence for a stereotyped and highly organized epitope map in the olfactory bulb. *Cell* 79, 1245–1255.
3. Vassar, R., Chao, S.K., Sitcheran, R., Nunez, J.M., Vosshall, L.B., and Axel, R. (1994). Topographic organization of sensory projections to the olfactory bulb. *Cell* 79, 981–991.
4. Clyne, P.J., Warr, C.G., Freeman, M.R., Lessing, D., Kim, J., and Carlson, J.R. (1999). A novel family of divergent seven-transmembrane proteins: Candidate odorant receptors in *Drosophila*. *Neuron* 22, 327–338.
5. Vosshall, L.B., Amrein, H., Morozov, P.S., Rzhetsky, A., and Axel, R. (1999). A spatial map of olfactory receptor expression in the *Drosophila* antenna. *Cell* 96, 725–736.
6. Gao, Q., Yuan, B., and Chess, A. (2000). Convergent projections of *Drosophila* olfactory neurons to specific glomeruli in the antennal lobe. *Nat. Neurosci.* 3, 780–785.
7. Vosshall, L.B., Wong, A.M., and Axel, R. (2000). An olfactory sensory map in the fly brain. *Cell* 102, 147–159.
8. Hildebrand, J.G., and Shepherd, G. (1997). Mechanisms of olfactory discrimination: Converging evidence for common principles across phyla. *Annu. Rev. Neurosci.* 20, 595–631.
9. Strausfeld, N.J., and Hildebrand, J.G. (1999). Olfactory systems: Common design, uncommon origins? *Curr. Opin. Neurobiol.* 9, 634–639.
10. Stocker, R.F. (2001). *Drosophila* as a focus in olfactory research: Mapping of olfactory sensilla by fine structure, odor specificity, odorant receptor expression and central connectivity. *Microsc. Res. Tech.* 55, 284–296.
11. Robertson, H.M., Warr, C.G., and Carlson, J.R. (2003). Molecular evolution of the insect chemoreceptor gene superfamily in *Drosophila melanogaster*. *Proc. Natl. Acad. Sci. USA* 100, 14537–14542.
12. Hallem, E.A., Ho, M.G., and Carlson, J.R. (2004). The molecular

- basis of odor coding in the *Drosophila* antenna. *Cell* 117, 965–979.
13. Laissue, P.P., Reiter, C., Hiesinger, P.R., Halter, S., Fischbach, K.F., and Stocker, R.F. (1999). Three-dimensional reconstruction of the antennal lobe in *Drosophila melanogaster*. *J. Comp. Neurol.* 405, 543–552.
  14. Bhalariao, S., Sen, A., Stocker, R.F., and Rodrigues, V. (2003). Olfactory neurons expressing identified receptor genes project to subsets of glomeruli within the antennal lobe of *Drosophila melanogaster*. *J. Neurobiol.* 54, 577–592.
  15. Fiala, A., Spall, T., Diegelmann, S., Eisermann, B., Sachse, S., Devaud, J.M., Buchner, E., and Galizia, C.G. (2002). Genetically expressed *cameleon* in *Drosophila melanogaster* is used to visualize olfactory information in projection neurons. *Curr. Biol.* 12, 1877–1884.
  16. Ng, M., Roorda, R.D., Lima, S.Q., Zemelman, B.V., Morcillo, P., and Miesenböck, G. (2002). Transmission of olfactory information between three populations of neurons in the antennal lobe of the fly. *Neuron* 36, 463–474.
  17. Wang, J.W., Wong, A.M., Flores, J., Vosshall, L.B., and Axel, R. (2003). Two-photon calcium imaging reveals an odor-evoked map of activity in the fly brain. *Cell* 112, 271–282.
  18. Yu, D., Ponomarev, A., and Davis, R.L. (2004). Altered representation of the spatial code for odors after olfactory classical conditioning: Memory trace formation by synaptic recruitment. *Neuron* 42, 437–449.
  19. Mombaerts, P., Wang, F., Dulac, C., Chao, S.K., Nemes, A., Mendelsohn, M., Edmondson, J., and Axel, R. (1996). Visualizing an olfactory sensory map. *Cell* 87, 675–686.
  20. Christensen, T.A., Waldrop, B.R., Harrow, I.D., and Hildebrand, J.G. (1993). Local interneurons and information processing in the olfactory glomeruli of the moth *Manduca sexta*. *J. Comp. Physiol. [A]* 173, 385–399.
  21. Sachse, S., and Galizia, C.G. (2002). Role of inhibition for temporal and spatial odor representation in olfactory output neurons: A calcium imaging study. *J. Neurophysiol.* 87, 1106–1117.
  22. Wilson, R.I., Turner, G.C., and Laurent, G. (2004). Transformation of olfactory representations in the *Drosophila* antennal lobe. *Science* 30, 366–370.
  23. Jefferis, G.S.X.E., Marin, E.C., Stocker, R.F., and Luo, L.L. (2001). Target neuron prespecification in the olfactory map of *Drosophila*. *Nature* 41, 204–208.
  24. Marin, E.C., Jefferis, G.S.X.E., Komiyama, T., Zhu, H., and Luo, L. (2002). Representation of the glomerular olfactory map in the *Drosophila* brain. *Cell* 109, 243–255.
  25. Wong, A.M., Wang, J.W., and Axel, R. (2002). Spatial representation of the glomerular map in the *Drosophila* protocerebrum. *Cell* 109, 229–241.
  26. Tanaka, N.K., Awasaki, T., Shimada, T., and Ito, K. (2004). Integration of chemosensory pathways in the *Drosophila* second-order olfactory centers. *Curr. Biol.* 14, 449–457.
  27. Itagaki, H., and Hildebrand, J.G. (1990). Olfactory interneurons in the brain of the larval sphinx moth *Manduca sexta*. *J. Comp. Physiol. [A]* 167, 309–320.
  28. Rodrigues, V. (1980). Olfactory behavior of *Drosophila melanogaster*. In *Development and Neurobiology of Drosophila*, O. Siddiqi, P. Babu, L.M. Hall, and J.C. Hall, eds. (New York and London: Plenum Press), pp. 361–371.
  29. Cobb, M. (1999). What and how do maggots smell? *Biol. Rev.* 74, 425–459.
  30. Heimbeck, G., Bugnon, V., Gendre, N., Häberlin, C., and Stocker, R.F. (1999). Smell and taste perception in *D. melanogaster* larva: Toxin expression studies in chemosensory neurons. *J. Neurosci.* 19, 6599–6609.
  31. Cobb, M., and Domain, I. (2000). Olfactory learning in individually assayed *Drosophila* larvae. *Proc. R. Soc. Lond. B. Biol. Sci.* 267, 2119–2125.
  32. Scherer, S., Stocker, R.F., and Gerber, B. (2003). Olfactory learning in individually assayed *Drosophila* larvae. *Learn. Mem.* 10, 217–225.
  33. Singh, R.N., and Singh, K. (1984). Fine structure of the sensory organs of *Drosophila melanogaster* Meigen larva (Diptera: Drosophilidae). *Int. J. Insect Morphol. Embryol.* 13, 255–273.
  34. Lee, T., and Luo, L. (1999). Mosaic analysis with a repressible cell marker for studies of gene function in neuronal morphogenesis. *Neuron* 22, 451–461.
  35. Tissot, M., Gendre, N., Hawken, A., Störckuhl, K.F., and Stocker, R.F. (1997). Larval chemosensory projections and invasion of adult afferents in the antennal lobe of *Drosophila melanogaster*. *J. Neurobiol.* 32, 281–297.
  36. Python, F., and Stocker, R.F. (2002). Adult-like complexity of the larval antennal lobe of *D. melanogaster* despite markedly low numbers of odorant receptor neurons. *J. Comp. Neurol.* 445, 374–387.
  37. Python, F., and Stocker, R.F. (2002). Immunoreactivity against choline acetyltransferase, gamma-aminobutyric acid, histamine, octopamine, and serotonin in the larval chemosensory system of *Drosophila melanogaster*. *J. Comp. Neurol.* 453, 157–167.
  38. Yang, M.Y., Armstrong, J.D., Vilinsky, I., Strausfeld, N.J., and Kaiser, K. (1995). Subdivision of the *Drosophila* mushroom bodies by enhancer-trap expression patterns. *Neuron* 15, 45–54.
  39. Stocker, R.F., Heimbeck, G., Gendre, N., and de Belle, J.S. (1997). Neuroblast ablation in *Drosophila* P[GAL4] lines reveals origins of olfactory interneurons. *J. Neurobiol.* 32, 443–456.
  40. Marin, E.C., Watts, R.J., Tanaka, N.J., Ito, K., and Luo, L.L. (2005). Developmentally programmed remodeling of the *Drosophila* olfactory circuit. *Development* 132, 725–737.
  41. Jefferis, G.S.X.E., Vyas, R.M., Berdnik, D., Ramaekers, A., Stocker, R.F., Ito, K., and Luo, L. (2004). Developmental origin of wiring specificity in the olfactory system of *Drosophila*. *Development* 13, 117–130.
  42. Ito, K., Suzuki, K., Estes, P., Ramaswami, M., Yamamoto, D., and Strausfeld, N.J. (1998). The organization of extrinsic neurons and their implications in the functional roles of the mushroom bodies in *Drosophila melanogaster* Meigen. *Learn. Mem.* 5, 52–77.
  43. Sun, X.J., Tolbert, L.P., and Hildebrand, J.G. (1997). Synaptic organization of the uniglomerular projection neurons of the antennal lobe of the moth *Manduca sexta*: A laser scanning confocal and electron microscopic study. *J. Comp. Neurol.* 379, 2–20.
  44. Yasuyama, K., Meinertzhagen, I.A., and Schürmann, F.W. (2002). Synaptic organization of the mushroom body calyx in *Drosophila melanogaster*. *J. Comp. Neurol.* 445, 211–226.
  45. Connolly, J.B., Roberts, I.J.H., Armstrong, J.D., Kaiser, K., Forte, M., Tully, T., and O’Kane, C.J. (1996). Associative learning disrupted by impaired G<sub>s</sub> signaling in *Drosophila* mushroom bodies. *Science* 274, 2104–2107.
  46. Zars, T., Fischer, M., Schulz, R., and Heisenberg, M. (2000). Localization of a short-term memory in *Drosophila*. *Science* 288, 672–674.
  47. Schwaerzel, M., Heisenberg, M., and Zars, T. (2002). Extinction antagonizes olfactory memory at the subcellular level. *Neuron* 35, 951–960.
  48. Lee, T., Lee, A., and Luo, L. (1999). Development of the *Drosophila* mushroom bodies: Sequential generation of three distinct types of neurons from a neuroblast. *Development* 126, 4065–4076.
  49. Troemel, E.R., Chou, J.H., Dwyer, N.D., Colbert, H.A., and Bargmann, C.I. (1995). Divergent seven transmembrane receptors are candidate chemosensory receptors in *C. elegans*. *Cell* 83, 207–218.
  50. Larsson, M.C., Domingos, A.I., Jones, W.D., Chiappe, M.E., Amrein, H., and Vosshall, L.B. (2004). *Or83b* encodes a broadly expressed odorant receptor essential for *Drosophila* olfaction. *Neuron* 4, 703–714.
  51. Rospars, J.P. (1983). Invariance and sex-specific variations of the glomerular organization in the antennal lobes of a moth, *Mamestra brassicae*, and a butterfly, *Pieris brassicae*. *J. Comp. Neurol.* 22, 80–96.
  52. Rospars, J.P., and Fort, J.C. (1994). Coding of odor quality: Roles of convergence and inhibition. *Network. Computation in Neural Systems* 5, 121–145.
  53. Lei, H., Christensen, T.A., and Hildebrand, J.G. (2004). Spatial and temporal organization of ensemble representations for different odor classes in the moth antennal lobe. *J. Neurosci.* 24, 11108–11119.

54. Strausfeld, N.J., Sinakevitch, I., and Vilinsky, I. (2003). The mushroom bodies of *Drosophila melanogaster*: An immunocytochemical and Golgi study of Kenyon cell organization in the calyces and lobes. *Microsc. Res. Tech.* 62, 151–169.
55. Livermore, A., Hutson, M., Ngo, V., Hadjisimos, R., and Derby, C.D. (1997). Elemental and configural learning and the perception of odorant mixtures by the spiny lobster *Panulirus argus*. *Physiol. Behav.* 62, 169–174.
56. Deisig, N., Lachnit, H., Sandoz, J.C., Lober, K., and Giurfa, M. (2003). A modified version of the unique cue theory accounts for olfactory compound processing in honeybees. *Learn. Mem.* 10, 199–208.
57. Heimbeck, G., Bugnon, V., Gendre, N., Keller, A., and Stocker, R.F. (2001). A central neural circuit for experience-independent olfactory and courtship behavior in *Drosophila melanogaster*. *Proc. Natl. Acad. Sci. USA* 98, 15336–15341.
58. Basler, K., and Struhl, G. (1994). Compartment boundaries and the control of *Drosophila* limb pattern by Hedgehog protein. *Nature* 368, 208–214.
59. Ramaekers, A., Parmentier, M.L., Lasnier, C., Bockaert, J., and Grau, Y. (2001). Distribution of metabotropic glutamate receptor DmGlu-A in *Drosophila melanogaster* central nervous system. *J. Comp. Neurol.* 438, 213–225.

#### Note Added in Proof

In a parallel study, Kreher et al. (2005) have shown that larval ORNs express essentially a single type of OR, together with the ubiquitously expressed OR83b, and that ORNs expressing different ORs target different LAL glomeruli. [Kreher, S.A., Kwon, J.Y., and Carlson, J.R. (2005). The molecular basis of odor coding in the *Drosophila* larva. *Neuron* 46, 445–456.]

This version differs from that published by Immediate Early Publication in that “n = 12” in column 2 of page 5 now reads n = 13/82. Also, one of the grant numbers was changed.